



HAL
open science

New advances on the *Brettanomyces bruxellensis* biofilm mode of life

Manon Lebleux, Hany Abdo, Christian Coelho, Louise Basmaciyani, Warren Albertin, Julie Maupeu, Julie Laurent, Chloé Roullier-Gall, Hervé Alexandre, Michèle Guilloux-Benatier, et al.

► To cite this version:

Manon Lebleux, Hany Abdo, Christian Coelho, Louise Basmaciyani, Warren Albertin, et al.. New advances on the *Brettanomyces bruxellensis* biofilm mode of life. *International Journal of Food Microbiology*, 2020, 318, pp.1-10. 10.1016/j.ijfoodmicro.2019.108464 . hal-02537081

HAL Id: hal-02537081

<https://hal.inrae.fr/hal-02537081v1>

Submitted on 21 Jul 2022

HAL is a multi-disciplinary open access archive for the deposit and dissemination of scientific research documents, whether they are published or not. The documents may come from teaching and research institutions in France or abroad, or from public or private research centers.

L'archive ouverte pluridisciplinaire **HAL**, est destinée au dépôt et à la diffusion de documents scientifiques de niveau recherche, publiés ou non, émanant des établissements d'enseignement et de recherche français ou étrangers, des laboratoires publics ou privés.



Distributed under a Creative Commons Attribution - NonCommercial 4.0 International License

1 New advances on the *Brettanomyces bruxellensis* biofilm mode of life

2

3 Manon Lebleux^a, Hany Abdo^a, Christian Coelho^b, Louise Basmaciyan^a, Warren Albertin^c, Julie
4 Maupeu^d, Julie Laurent^a, Chloé Roullier-Gall^a, Hervé Alexandre^a, Michèle Guilloux-Benatier^a,
5 Stéphanie Weidmann^a, Sandrine Rousseaux^{a#}

6

7 ^aUniv. Bourgogne Franche-Comté, AgroSup Dijon, PAM UMR A 02.102 Dijon-France.
8 Laboratoire VALMiS-IUVV

9 ^bUniv. Bourgogne Franche-Comté, AgroSup Dijon, PAM UMR A 02.102 Dijon-France.
10 Laboratoire PCAV

11 ^cUSC 1366 INRA, Institut des Sciences de la Vigne et du Vin, Unité de Recherche Œnologie EA
12 4577, University of Bordeaux, Bordeaux, France

13 ^dMicroflora-ADERA, Institut des Sciences de la Vigne et du Vin, Unité de Recherche Œnologie
14 EA 4577, Bordeaux, France

15

16 Current e-mail addresses of the co-authors:

17 Manon Lebleux: Manon.Lebleux@u-bourgogne.fr

18 Hany Abdo: hany.abdo@u-bourgogne.fr

19 Christian Coelho: christian.coelho@u-bourgogne.fr

20 Louise Basmaciyan: louise.basmaciyan@u-bourgogne.fr

21 Warren Albertin: warren.albertin@u-bordeaux.fr

22 Julie Maupeu : julie.maupeu@u-bordeaux.fr

23 Julie Laurent : julie.laurent@u-bourgogne.fr

24 Chloé Roullier-Gall : Chloe.Roullier-Gall@u-bourgogne.fr

- 25 Hervé Alexandre : rvalex@u-bourgogne.fr
- 26 Michèle Guilloux-Benatier : michele.guilloux-benatier@u-bourgogne.fr
- 27 Stéphanie Weidmann: stephanie.weidmann@u-bourgogne.fr
- 28 Sandrine Rousseaux: sandrine.rousseaux@u-bourgogne.fr
- 29
- 30 #Corresponding author: Sandrine Rousseaux
- 31
- 32 Manon Lebleux and Hany Abdo contributed equally to this work

33 **ABSTRACT**

34 The wine spoilage yeast *Brettanomyces bruxellensis* can be found at several steps in the
35 winemaking process due to its resistance to multiple stress conditions. The ability to form biofilm
36 is a potential resistance strategy, although it has been given little attention so far for this yeast. In
37 this work, the capacity to form biofilm and its structure were explored in YPD medium and in
38 wine. Using microsatellite analysis, 65 isolates were discriminated into 5 different genetic groups
39 from which 12 strains were selected. All 12 strains were able to form biofilm in YPD medium on
40 a polystyrene surface. The presence of microcolonies, filamentous cells and extracellular
41 polymeric substances, constituting the structure of the biofilm despite a small thickness, were
42 highlighted using confocal and electronic microscopy. Moreover, different cell morphologies
43 according to genetic groups were highlighted. The capacity to form biofilm in wine was also
44 revealed for two selected strains. The impact of wine on biofilms was demonstrated with firstly
45 considerable biofilm cell release and secondly growth of these released biofilm cells, both in a
46 strain dependent manner. Finally, *B. bruxellensis* has been newly described as a producer of
47 chlamyospore-like structures in wine, for both planktonic and biofilm lifestyles.

48

49 **Keywords:** *Brettanomyces*, spoilage microorganism, microcolonies, chlamyospore, wine

50 **1. INTRODUCTION**

51 Biofilms are complex associations of single- and multiple- species interconnected cells embedded
52 in a hydrated self-produced matrix established at a solid/liquid or liquid/air interfaces (Alexandre,
53 2013; Costerton et al., 1995; Hall-Stoodley et al., 2004; Kolter and Greenberg, 2006). Biofilm
54 development is a dynamic process including the key steps of the adhesion and maturation of
55 microcolonies in a three-dimensional structure, and detachment during which cells acquire a
56 particular phenotype (Flemming and Wingender, 2010; Sauer et al., 2002). Extracellular
57 polymeric substances (EPS) produced throughout biofilm development are mainly composed of
58 polysaccharides, proteins, extracellular DNA (eDNA) and lipids (Flemming, 2016; Jachlewski et
59 al., 2015; Zarnowski et al., 2014) and can be present at various quantities dependent on
60 environmental conditions, the age of the biofilm and the type of microorganisms involved (Mayer
61 et al., 1999). Biofilm mode of life allows microorganisms to better adapt to environmental
62 conditions through metabolic cross-feeding, cell–cell interactions and especially chemical and
63 physical resistance (Bastard et al., 2016; Davey and O’toole, 2000; O’Connell et al., 2006). This
64 growth strategy, through surface colonization and the increase of stress resistance, contributes to
65 the persistence of microorganisms in different environments, such as those encountered in the
66 food industry (Coenye and Nelis, 2010; Møretrø and Langsrud, 2017). In some cases, biofilms
67 are used for increased microorganism performance, for example in the production of ethanol
68 (Germec et al., 2016), their involvement in fermentation processes and persistence in the wine
69 environment (Bastard et al., 2016; Tek et al., 2018). However, many studies have investigated the
70 presence of biofilms, especially in the case of negative effects due to the risk of recurrent
71 contamination of food and raw materials by pathogenic or spoilage species (Alvarez-Ordóñez et
72 al., 2019; Bridier et al., 2015). By studying biofilms present on the process surfaces of breweries,

73 different spoilage microorganisms as *Acinetobacter*, *Bacillus*, *Citrobacter*, *Pseudomonas*,
74 *Saccharomyces cerevisiae* and *Candida pelliculosa* were isolated (Timke et al., 2008, 2004).
75 In the wine industry, one of the most feared spoilage microorganisms is the yeast *Brettanomyces*
76 *bruxellensis*. This yeast is responsible for the production of volatile phenols and most importantly
77 4-ethylphenol, which contributes to undesirable aromas described as “Brett character” (Chatonnet
78 et al., 1992; Oelofse et al., 2008; Wedral et al., 2010), leading to rejection by consumers and to
79 heavy economic losses (Fugelsang, 1997; Lattey et al., 2010). This yeast can be found at several
80 steps in the winemaking process (Chatonnet et al., 1992; Renouf et al., 2009, 2006; Renouf and
81 Lonvaud-Funel, 2007; Rubio et al., 2015; Suárez et al., 2007) due to its resistance to multiple
82 stress conditions (Avramova et al., 2018b; Conterno et al., 2006; Longin et al., 2016;
83 Schifferdecker et al., 2014; Serpaggi et al., 2012; Smith and Divol, 2016). The ability to form
84 biofilm is another potential resistance strategy (Tek et al., 2018; Verstrepen and Klis, 2006),
85 although in the case of *B. bruxellensis* it has been given only little attention so far. Up to now,
86 few studies have demonstrated the capacity of several strains of *B. bruxellensis* to adhere on
87 several surfaces (Ishchuk et al., 2016; Joseph et al., 2007; Kregiel et al., 2018; Poupault, 2015;
88 Tristezza et al., 2010). Thus, Joseph et al. (2007) pinpointed for the first time the capacity of *B.*
89 *bruxellensis* isolates to adhere and form a biofilm-like structure on polystyrene surfaces; also, the
90 biofilm structures were not described. Moreover, the efficiency of adhesion and biofilm-like
91 formation depend on the nutritional environment (Kregiel et al., 2018; Tristezza et al., 2010).
92 Although these studies demonstrated the ability of *B. bruxellensis* to adhere and form a biofilm-
93 like film, there is a lack of microscopic observations of these biofilm-like structures in synthetic
94 media and in wine. Such observations would highlight the three-dimensional structure of the film
95 and EPS production. Using confocal microscopy, Poupault (2015) was alone in describing
96 different adhesion capacities with three-dimensional structures on polystyrene. Therefore, it

97 seems necessary to deepen knowledge on the adhesive and biofilm formation capacities of *B.*
98 *bruxellensis*, and to demonstrate its ability to form a biofilm (*i.e.* thickness, presence of
99 microcolonies, EPS) on different surfaces in view to achieving better subsequent removal of this
100 microbial species from winemaking material.

101 In this context, the purpose of our study was to: (i) investigate the kinetics of biofilm formation
102 of *B. bruxellensis* strains; (ii) visualise the biofilm structure and morphology of cells by
103 microscopic observations; and (iii) investigate the behaviours of biofilm in wine.

104 **2. MATERIAL AND METHODS**

105 **2.1. Yeast isolates**

106 A total of 65 isolates belonging to the yeast *B. bruxellensis* were used in this study. These isolates
107 were obtained from enological materials (*i.e.* from barrels, taps, pipes, transfer tanks) and/or wine
108 from a winery. The yeasts were stored at -80°C in YPD liquid medium (0.5% w/v yeast extract
109 (Biokar, Beauvais, France), 1% w/v bactopectone (Biokar), 2% w/v D-glucose (Prolabo,
110 Fontenay-sous-Bois, France) and 0.02% w/v chloramphenicol (Sigma, St Louis, USA)),
111 containing 20% (v/v) glycerol.

112

113 **2.2. Genotyping by microsatellite analysis**

114 The DNA extraction of *B. bruxellensis* strain and PCR conditions for the microsatellite markers
115 amplification and the amplicon analysis were performed according to Albertin et al., 2014 and
116 Avramova et al., 2018a. Briefly, twelve microsatellite regions were amplified from the DNA of
117 the 65 isolates, then fragment length was analyzed by capillary electrophoresis on an ABI 3130
118 XL sequencing machine (Albertin et al., 2014). A number of repeated patterns for each
119 microsatellite region analyzed were associated for each isolate. The diversity of the isolates
120 studied was determined according to the variability of the number of repetitions.

121 To investigate the genetic relationships between strains, the microsatellite data-set was analyzed
122 using the *Poppr* package in R. A dendrogram was established using Bruvo's distance and
123 Neighbour Joining (NJ) clustering (Bruvo et al., 2004; Kamvar et al., 2014; Paradis et al., 2004).
124 Bruvo's distance takes into account the mutational process of microsatellite loci and is well
125 adapted to populations with mixed ploidy levels and is therefore, suitable for the study of the *B.*
126 *bruxellensis* strain collection used in this work.

127 Clones were defined as isolates displaying the same genotype for all 12 microsatellite markers
128 tested, allowing the generation of clonal groups.

129

130 **2.3. Biofilm formation in YPD medium**

131 **2.3.1. YPD cultures**

132 Using cultures stored at -80°C, starter cultures were prepared in triplicate in 5 mL of YPD
133 medium at 28°C for 6 days. Then, the starter cultures were passed twice into fresh medium to
134 obtain cultures in the same physiological state. Then, cell suspensions were readjusted at OD_{600nm}
135 = 0.05 ($1 OD_{600nm} = 1.0 \times 10^7$ CFU/mL) in YPD medium to obtain the “YPD working culture”.

136 **2.3.2. Biofilm formation on polystyrene plates**

137 Twelve strains were selected from the 5 genetic groups, taking into account the distribution of the
138 clonal groups. For each of the 12 strains selected, the biofilm formation on the polystyrene
139 microplate was evaluated according to (Rieu et al., 2007) and adapted to the yeast. One mL of the
140 “YPD working culture” was inoculated in 3 technical and 3 biological repetitions in a 24-well
141 polystyrene plate from Costar® (Corning Incorporated, New-York, USA) at 28°C. After 48 hours
142 and 7, and 14 days (with medium turnover every 3.5 days), the wells were carefully washed twice
143 with 500µL of sterile physiological water (0.9% NaCl) to eliminate non-adhered cells. With the
144 addition of 1 mL of sterile physiological water, the adhered cells were detached by strong
145 pipetting with 15 backflows. The detached cells were estimated by numbering on YPD plates
146 (YPD broth with 2% w/v agar) at 28°C after serial dilutions.

147

148 **2.4. Biofilm formation in wine**

149 **2.4.1. Wine used**

150 The wine used was elaborated from the Pinot Noir grape variety (Marsannay, 2018 vintage). This
151 red wine was characterized by 11.20% (v/v) ethanol and a pH of 3.45. The wine was filtered and
152 sterilized using a vacuum driven filtration system through a 0.22 µm sterile membrane (Stericup-
153 GP, polyethersulfone, SCGPU05RE, Millipore Express® Plus Membrane).

154 **2.4.2. Culture adaptation**

155 Two different strains with significantly different number of adhered cells on polystyrene in YPD
156 medium at 14 days (strains 11 and 14) were selected to study biofilm formation in wine. Before
157 planktonic cell incubation in wine, the cells were adapted in wine as previously described
158 (Longin et al., 2016). Using cultures stored at -80°C, starter cultures were prepared in triplicate in
159 YPD medium at 28°C for 6 days. The cultures were therefore incubated in 10 mL of YPD
160 medium supplemented with 5% (v/v) ethanol for 48h. The OD_{600nm} of each culture was adjusted
161 to 0.1 into a 50:50 (v/v) wine:water solution. After wine adaptation, the cell concentration was
162 readjusted to 5.0×10⁵ CFU/mL in the wine to obtain the “wine working culture”.

163 **2.4.3. Biofilm formation on stainless steel chips in wine**

164 The biofilm formation of *B. bruxellensis* in wine was studied on stainless steel chips using a
165 protocol previously described (Bastard et al., 2016) and adapted to the yeasts. Briefly, stainless-
166 steel chips (25 mm × 25 mm, Goodfellow, 316L, France) were immersed in 13 mL of the “wine
167 working culture” described in paragraph 2.4.2. and incubated for at 28°C. The yeast population
168 was monitored on the chip (*i.e.* cells adhered and developed into biofilm): after 2, 24, 48 hours, 7
169 and 14 days of incubation, the chips were collected and rinsed for 30 seconds in 13 mL of sterile
170 physiological water to eliminate non-adhered cells on the chips. Afterwards, the chips were
171 placed in new sterile physiological water (13 mL) and the cells were detached by sonication (3
172 min) (Branson CPXH1800H-E; Branson Ultrasonic Corporation, Danbury, USA). For each
173 time point, the cells detached from the chips were numbered by plating on YPD plates at 28°C

174 after serial dilutions. This experiment was performed in biological triplicates for each strain (*i.e.*
175 3 different “wine working cultures”).

176 **2.4.4. Wine effect on 7 day-aged biofilms**

177 For selected strains 11 and 14, the 7 day-aged biofilm formed on stainless-steel chips was
178 obtained from the “YPD working culture” as previously described in paragraph 2.4.3. Then, the
179 stainless-steel chips were placed in the sterile wine (13 mL) and the evolution of the yeast
180 population on the chip (*i.e.* biofilm cells) and in the wine (*i.e.* planktonic cells, corresponding to
181 cells released from biofilm over the time) was monitored. The 7 day-aged biofilm formed on
182 stainless-steel chips was incubated at 28°C for 2, 24, 48 hours and 7 and 14 days and treated as
183 described in paragraph 2.4.3. For each time point, the cells detached from the chips and the cells
184 contained in the wine were numbered by plating on YPD plates at 28°C after serial dilutions. This
185 experiment was performed in biological triplicates for each strain (*i.e.* 3 different “YPD working
186 cultures”).

187

188 **2.5. Cell observations**

189 **2.5.1. Confocal Laser Scanning Microscopy (CLSM)**

190 From the “YPD working culture”, 7 day-aged biofilms (with a medium turnover at 3.5 days) were
191 formed in a 96-well polystyrene plate from Cellstar® (Greiner Bio-One International,
192 Kremsmünster, Austria). After 7 days, each well was carefully washed with 100µL of MacIlvaine
193 Buffer containing 2.83% w/v sodium phosphate dibasic (Sigma, St. Louis, USA), 2.10% w/v
194 citric acid monohydrate (Sigma, St. Louis, USA) and adjusted at pH 4.0. Surface-associated cells
195 were fluorescently tagged by adding 5(6)-Carboxyfluorescein Diacetate (CFDA) esterase activity
196 marker (green; $\lambda_{ex} = 495 \text{ nm} / \lambda_{em} = 520 \text{ nm}$) at 7.5 µM (ThermoFisher, Illkrich, France) and the
197 plate was placed in a dark place for 15 minutes.

198 The surface associated-cells were examined using a Leica TCS SP8 (Leica Microsystems,
199 Germany) inverted confocal laser scanning microscope at the DImaCell Platform
200 (<http://dimacell.fr/index.php>). Observations were performed using a 40×/1.25 oil immersion
201 objective lens. CLSM was equipped with a solid 488 nm diode (laser power: 3%) and the
202 fluorescence emitted was recorded from 500 to 554 nm using a PMT detector with a gain of
203 790V. The images were acquired by LAS X software (Leica Microsystems, Germany) at a
204 resolution of 1024×1024 pixels, a scan speed of 400Hz and a line average of 2. To assess the
205 thickness of the structure and obtain 3D views, a series of optical sections at 1- μ m intervals in the
206 z-axis were taken throughout the full depth of the sample. The bright field channel was acquired
207 simultaneously, using a second PMT detector. Subsequently, 3D reconstruction images of the
208 biofilms were generated with LAS X software to obtain a top view for each strain.
209 ImageJ software was used to determine cell morphology and biofilm thickness from CLSM
210 images. For the cell morphology, the length to width (l/w) ratio and cell area were determined
211 from fifty measurements of single cells (Basmacıyan et al., 2018). For biofilm thickness, 5
212 random cuts following the z-axis were performed for each of the strains studied and 10
213 measurements were made per cut (total 50 measurements by strain).

214 **2.5.2. Scanning Electron Microscopy (SEM)**

215 Biofilms were formed on stainless steel chips from the “YPD working culture” (for 7 days) and
216 from “wine working culture” (for 7 and 14 days). The cells were fixed directly on the stainless-
217 steel chips by a solution of 3% glutaraldehyde in 0.1 M phosphate buffer of pH 7.2 for 3 hours at
218 4°C. The samples were then washed with 0.05 mM phosphate buffer for 10 min at room
219 temperature. Dehydration was performed by two successive immersions for 10 min in solutions
220 of increasing ethanol content (30, 50, 70, 90, 100%). Then, each mixture was placed in a bath of
221 ethanol-acetone solution (70:30, 50:50, 30:70, 100%) for 10 min. The chips were then air-dried

222 and stored at room temperature. Afterwards, the samples were coated with a thin gold layer using
223 an Edwards Scancoat Six Pirani 201 sputter coater (Edwards High Vacuum, Crawley, England)
224 and then observed with a Hitachi SU1510 scanning electron microscope (Hitachi High-
225 Technologies Corporation, Japan). SEM was performed at an accelerating voltage of 15 kV using
226 a working distance between 7.5 mm and 9.7 mm.

227 **2.5.3. Epifluorescence microscopy**

228 Planktonic cells were incubated from the “wine working culture” at 28°C for 14 days. The cells
229 were adhered on a microscope fluorescence slide and then fixed in methanol at room temperature
230 for 5 minutes. The fungal cell wall was stained using the Fungi-Fluor® kit (calcofluor)
231 (Polysciences, Inc., Warrington, PA) according to the manufacturer's protocol. Briefly, samples
232 were incubated for 5 minutes with the reagent and washed once in Phosphate Buffer Saline 1×
233 before adding a coverslide. The slides were examined with a BX51 epifluorescence microscope
234 (Olympus, Rungis, France) coupled with the “CellF” software and using an “UPlanFL 40×”
235 objective.

236

237 **2.6. Statistical analyses**

238 All the assays were performed in three biological replicates. The biomass and biofilm thickness
239 data are expressed as means, assigned with the standard deviation. A one-way analysis of
240 variance (ANOVA) with a post-hoc Tukey Honestly Significant Difference (HSD) test was used
241 for statistical comparison. A p-value ≤ 0.05 was considered statistically significant. For cell
242 morphology, the same test was used for the comparison of areas A, B and C with p-values ≤ 0.01 .

243 3. RESULTS

244

245 3.1. Biofilm structures

246 Sixty-five isolates of *B. bruxellensis* from enological materials (*i.e.* from barrels, taps, pipes,
247 transfer tanks) and/or wine from a winery were discriminated by microsatellite analysis allowing
248 their distribution in 5 of the 6 genetic groups (GG) described by Avramova et al., 2018a. The
249 majority of isolates belong to GG3 and none belongs to the GG5 (Table 1). In all, 34 clonal
250 groups were formed (each including isolates with a genetic distance equal to zero) (Table 1),
251 allowing the selection of twelve strains distributed among the 5 genetic groups. Their ability to
252 form biofilm in YPD medium was studied.

253 Biofilm formation kinetics was monitored in three independent biological replicates at 3 different
254 time points: 48 hours, 7 days and 14 days on polystyrene microplates for the 12 strains selected
255 (Table 2). At 48h, the different strains presented an average adhered population around 3.3×10^6
256 CFU/cm², except strains 11, 20, 60 and 63, which had a statistically lower population around
257 5.5×10^5 CFU/cm². At 7 days, the adhered population distribution ranged between 6.9×10^5 and
258 6.3×10^6 CFU/cm². Statistically, strains 2 and 65 had a larger adhered population compared to
259 strains 7, 9, 11, 14, 20, 36 and 63. At 14 days, the populations of the 12 strains reached an
260 average biomass of 4.1×10^6 CFU/cm². Strain 11 presented a significantly lower quantity of
261 adhered cells compared to strains 7, 9, 14, 20, and 36 (Table 2).

262 Seven day-aged biofilms for the 12 strains were observed by CLSM to investigate biofilm
263 characteristics (Fig. 1). CLSM observations showed cellular layers covering the entire surface for
264 all the strains, except strain 63 which presented some uncovered areas. For this strain, the surface
265 coverage seemed to be different with the development of microcolonies instead of cell layers
266 spreading over the surface (Fig. 1A).

267 Biofilm thickness was determined for each strain. Average thickness values were obtained from
268 50 measurements of random biofilm cuts of the representative views (Fig. 1A). An average
269 thickness of 9.45 μm was measured throughout the 12 strains. Taken together, these data suggest
270 that all the strains tested were able to develop in contact with a surface. It is also noteworthy that
271 the thickness of the biofilm appears to be related to cell size (Fig. 1A). Indeed, magnifications of
272 the CLSM images performed for each strain allowed observing different cell shapes such as
273 “round”, “lemon”, “rice grain” or “elongated” according to the strains (Fig. 1A, Table 3). In
274 addition, filamentous cells were observed (Fig. 1B).

275 To better characterize these different cell shapes, the length to width ratio (l/w) and cell area were
276 determined for 50 individual cells per strain (Basmacıyan et al., 2018). Each genetic group was
277 characterized by its own cell measurements and cell shape (Table 3). The strains of GG1 were
278 characterized by a “round” shape with an average cell area of 15.72 μm^2 and average l/w ratio of
279 1.55, except strain 61 which presented a “rice grain” shape with atypical measurements of 12.75
280 μm^2 and 1.91, respectively. The strains of GG2 with a “rice grain” shape were characterized by
281 an average cell area of 11.36 μm^2 and average l/w ratio of 1.91. The strains of GG3 were
282 characterized by an “elongated” shape with an average cell area of 16.5 μm^2 and an average l/w
283 ratio of 2.53. Strain GG4 was characterized by a “lemon” shape with a cell area of 16.03 μm^2 and
284 a l/w ratio of 2.08. Finally, the “round” shaped cells of GG6 presented an average cell area of
285 16.57 μm^2 and an average l/w ratio of 1.50. The distribution of the 12 strains according to cell
286 area determined as a function of l/w ratio (Fig. 2), showed that the strains were statistically
287 distributed in 3 different areas corresponding to morphological cell characteristics. GG3 and GG4
288 (area A) were grouped together as were GG6 and GG1 (area B), with the exception of strain 61.
289 Indeed, this strain was statistically grouped with GG2 (area C). These results suggest a link
290 between genetic groups and cell morphology.

291 Although CLSM provided an overview of the cells adhered on polystyrene, additional SEM
292 observations were necessary to demonstrate and validate characteristic structures of biofilm
293 development. Observations of strains 11 and 14 developed for 7 days on the stainless-steel chips
294 in YPD medium (Fig. 3A) revealed the presence of microcolonies containing cells embedded in
295 EPS and filamentous cells possibly playing a role in their cohesion.

296

297 **3.2. *Brettanomyces* biofilm mode of life: what's up in wine?**

298 The ability of the both strains (11 and 14) of *B. bruxellensis* were then investigated in wine to
299 study (i) the development into biofilm in wine and (ii) the impact of wine on an established *B.*
300 *bruxellensis* biofilm. These strains were chosen for their different ability to adhere on polystyrene
301 (Table 2).

302 Firstly, in order to confirm the ability of both strains to form biofilm in wine, SEM observations
303 at 7 days were realized (Fig. 3B). Once again, the capacity of both strains to adhere and form
304 microcolonies surrounded by EPS was demonstrated as well as the presence of filamentous cells,
305 suggesting the beginning of a biofilm structure development. However, strain 14 presented only a
306 few microcolonies scattered on the chips: adhesion and microcolony formation of strain 14 were
307 more affected by the wine than strain 11. The *B. bruxellensis* cell growth on stainless steel chips
308 was monitored in wine from 2 hours to 14 days (Fig. 4). Strain 14 had a weak adhesion rate of
309 0.69% at 2 hours compared to strain 11 (5.69%). This difference is maintained between the both
310 strains until 7 days. However, after 2 hours, for the both strains no growth was observed.

311 Secondly, the impact of wine on an established *B. bruxellensis* biofilm was investigated. A 7 day-
312 aged biofilm (previously developed on stainless steel chips in YPD medium) was immersed in
313 wine for enumeration of cells (i) on the chips and (ii) released into the wine (Fig. 5). For both
314 strains, the amount of cells adhered on the stainless steel chip significantly decreased at 24 hours

315 and then remains stable for up to 14 days (Fig. 5A and 5B). As previously described, strain 14
316 was more affected by the wine than strain 11. Moreover, as early as 2 hours, the impact of wine
317 on biofilm led to the release of cells from chip with around 10^6 CFU/mL for the both strains (Fig.
318 5C and 5D). For strain 14, a decrease in the number of released cells was observed as early as 24
319 hours before remaining stable up to 7 days. Then, a growth recovery was observed at 14 days.
320 The same behaviour was observed for strain 11 in a lesser extent.

321

322 **3.3.Chlamyospore-like structure, a new piece of *B. bruxellensis* morphotype**

323 Finally, SEM observations of 14 day-aged microcolonies of strain 11 in wine allowed observing
324 specific round, large and free shaped cells (Fig. 6A). These structures are consistent with the
325 definition of a chlamyospore, a morphological structure defined as larger than a yeast cell,
326 highly refractile cells with thick walls derived from filamentous cells (Staib and Morschhäuser,
327 2007). Chlamyospore walls are composed by chitin, which can be stained by the calcofluor
328 (Martin et al., 2005). Thus, the use of this staining coupled with epifluorescence microscopy
329 observations allowed to reveal very refractive rounded structures with a thick wall for both strains
330 11 and 14 grown for 14 days in wine (Fig. 6B).

331 4. DISCUSSION

332 The ability of microorganisms to form biofilm has been pinpointed out (Bastard et al., 2016) as
333 one of the strategies of withstanding wine stresses. Up to now, few studies have highlighted the
334 capacity of *B. bruxellensis* to develop into biofilm-like structure (Ishchuk et al., 2016; Joseph et
335 al., 2007; Kregiel et al., 2018; Poupault, 2015; Tristezza et al., 2010). The analysis methods used
336 staining method associated with OD measurement, luminometry or Calgary Biofilm Device
337 system (MBEC™ P & G assay). The first methods are rapid but quite imprecise. The latter,
338 allowing the enumeration of *B. bruxellensis* biofilm-like structures in CFU/peg, could not be
339 compared with the other methods of biofilm quantification. However, none of these studies
340 described the structure of biofilm formed by *B. bruxellensis* using microscopy, except Poupault
341 (2015). For the present study, a protocol adapted from an established method of numbering
342 bacterial biofilm populations (Bastard et al., 2016) was developed to study the biofilm formation
343 of *B. bruxellensis* yeast on different supports such as polystyrene plates and stainless steel chips.
344 Cells were placed in the same physiological state, allowing to compare the capacity of different
345 strains to form a biofilm (Bastard et al., 2016; Rieu et al., 2014; Stepanović et al., 2007).
346 Moreover, microscopic observations of biofilm structures have been performed to obtain better
347 insight into the biofilm structure of *B. bruxellensis*. The both microscopy methods used highlight
348 different points. CLSM allowed notably to gain information on the shape of the cells and the
349 thickness of the biofilm-like structure while SEM enable to observe easily different cell structures
350 (*i.e.* cells, filaments, chlamydo spores) and EPS. The 7 day-aged biofilms formed by the *B.*
351 *bruxellensis* strains studied in this work had an average thickness of 9.45 µm, which is rather thin
352 compared to biofilms described for other yeast species (Bojsen et al., 2014). However, *Candida*
353 *albicans* biofilms reach thicknesses ranging from 8 to 84 µm depending on the surrounding
354 environment (Daniels et al., 2013; Nweze et al., 2012). Other yeasts such as *S. cerevisiae* and

355 *Rhodotorula mucilaginosa* presented only microcolonies without any multi-layered architecture
356 (Andersen et al., 2014; Nunes et al., 2013).

357 In this work, CLSM and SEM observations revealed the presence of several filamentous cells that
358 appeared to start from the base of the biofilm and extend upward, suggesting the beginning of a
359 multilayer structure. Similar organizations have been identified in biofilms of *C. albicans* and *C.*
360 *tropicalis* with a basal layer composed of yeast cells and an upper layer composed of filamentous
361 cells collectively embedded in an extracellular matrix (Daniels et al., 2013; Jones et al., 2014;
362 Park et al., 2017).

363 Among *B. bruxellensis* morphological features, the specific cell morphology observed in biofilm
364 (based on cell area, length and width measurements) could be related to the genetic group
365 (determined by Avramova et al., 2018a), even if it need to be confirmed with a larger number of
366 strains.

367 Since *B. bruxellensis* is the major spoilage yeast of wine, it was crucial to enrich the information
368 available on its capacity to form biofilms in enological environments. So, 2 strains of *B.*
369 *bruxellensis* with different morphologies and different capacities to form biofilm in YPD medium
370 were selected. Both strains were able to form microcolonies on stainless steel chips in wine even
371 if strain 14 showed lower adhesion and development at 2 weeks than strain 11. Stressful
372 environment of wine had also a strong impact on 7 day-aged microcolonies with cell release in a
373 strain-dependent manner. After a decrease of cell population released in wine, probably due to
374 cell death and/or to the entry in viable but non culturable (VBNC) state (Serpaggi et al., 2012),
375 growth restarted after several days. As described for other microorganisms, the biofilm mode of
376 life may allow *Brettanomyces* to persist in wine and wine-related environments (Bastard et al.,
377 2016). The role of EPS in stress resistance as a function of their nature and proportion in the
378 matrix has been highlighted in several microorganisms (Flemming and Wingender, 2010). By

379 observing EPS in *B. bruxellensis* biofilm, this study provides the basis for new fields of
380 investigation into the resistance of *B. bruxellensis*. No data being available on EPS in *B.*
381 *bruxellensis* biofilm, it will be necessary to identify the chemical nature of the EPS and then
382 study their specific role in stress resistance mechanisms.

383
384 Finally, microscopic observations of planktonic and biofilm cultures in wine unexpectedly
385 revealed the presence of “chlamyospore-like” structures that have never been observed for *B.*
386 *bruxellensis*. We observed structures larger than a yeast cell, highly refractile with thick walls and
387 derived from filamentous cells. Such characteristics were reported for the description of
388 chlamyospore-like structures in *C. albicans* (Martin et al., 2005; Navarathna et al., 2016; Staib
389 and Morschhäuser, 2007), *Cryptococcus neoformans* (Lin and Heitman, 2005) and the close
390 relatives *C. albicans* and *C. dubliniensis* cultured in planktonic or biofilm conditions (Boucherit-
391 Atmani et al., 2011; Citiulo et al., 2009; Staib and Morschhäuser, 2007). Chlamyospores were
392 described as forms of resistance in some fungi like *Duddingtonia flagrans* (Ojeda-Robertos et al.,
393 2009) or *Gibberella zeae* (Son et al., 2012), however in yeast, their role was never clearly
394 identified, although a potential role in the long-term survival of *C. albicans* within the host or in
395 resistance to host immunity was hypothesized (Navarathna et al., 2016; Staib and Morschhäuser,
396 2007). So, future works should be carried out to determine the role of these “chlamyospore-like”
397 structures for *Brettanomyces* yeast.

398 **ACKNOWLEDGEMENTS**

399 The authors would like to thank the Dimacell Imaging Facility, Agrosup Dijon, INRA, INSERM,
400 Univ. Bourgogne Franche-Comté, F-21000 Dijon France" and Marie-Laure Léonard and Jean-
401 Marc Dachicourt (ESIREM, Université de Bourgogne, Dijon, France) for their technical
402 assistance for the microscopic observations, and IFV Beaune and Nexidia SAS for providing *B.*
403 *bruxellensis* strains.

404

405 **FUNDING SOURCES**

406 This work was supported by the Regional Council of Bourgogne- Franche-Comté and the “Fonds
407 Européen de Développement Régional (FEDER)” [CRB 2016-9201AAO048S01632]; the
408 "Bureau Interprofessionnel des Vins de Bourgogne (BIVB)" [CONV1617_04] and the Ministère
409 de l’Enseignement supérieur, de la Recherche et de l’Innovation.

410 **REFERENCES**

- 411 Albertin, W., Panfili, A., Miot-Sertier, C., Goulielmakis, A., Delcamp, A., Salin, F., Lonvaud-
412 Funel, A., Curtin, C., Masneuf-Pomarede, I., 2014. Development of microsatellite markers
413 for the rapid and reliable genotyping of *Brettanomyces bruxellensis* at strain level. Food
414 Microbiol. 42, 188–195. <https://doi.org/10.1016/j.fm.2014.03.012>
- 415 Alexandre, H., 2013. Flor yeasts of *Saccharomyces cerevisiae*-Their ecology, genetics and
416 metabolism. Int. J. Food Microbiol. 167, 269–275.
417 <https://doi.org/10.1016/j.ijfoodmicro.2013.08.021>
- 418 Alvarez-Ordóñez, A., Coughlan, L.M., Briandet, R., Cotter, P.D., 2019. Biofilms in Food
419 Processing Environments: Challenges and Opportunities. Annu. Rev. Food Sci. Technol. 10,
420 173–195. <https://doi.org/10.1146/annurev-food-032818-121805>
- 421 Andersen, K.S., Bojsen, R., Sørensen, L.G.R., Nielsen, M.W., Lisby, M., Folkesson, A.,
422 Regenbergs, B., 2014. Genetic basis for *Saccharomyces cerevisiae* biofilm in liquid medium.
423 G3 Genes, Genomes, Genet. 4, 1671–1680. <https://doi.org/10.1534/g3.114.010892>
- 424 Avramova, M., Cibrario, A., Peltier, E., Coton, M., Coton, E., Schacherer, J., Spano, G., Capozzi,
425 V., Blaiotta, G., Salin, F., Dols-Lafargue, M., Grbin, P., Curtin, C., Albertin, W., Masneuf-
426 Pomarede, I., 2018a. *Brettanomyces bruxellensis* population survey reveals a diploid-triploid
427 complex structured according to substrate of isolation and geographical distribution. Sci.
428 Rep. 8, 4136. <https://doi.org/10.1038/s41598-018-22580-7>
- 429 Avramova, M., Vallet-Courbin, A., Maupeu, J., Masneuf-Pomarède, I., Albertin, W., 2018b.
430 Molecular diagnosis of *Brettanomyces bruxellensis*' sulfur dioxide sensitivity through
431 genotype specific method. Front. Microbiol. 9, 1260.
432 <https://doi.org/10.3389/fmicb.2018.01260>
- 433 Basmaciyan, L., Berry, L., Gros, J., Azas, N., Casanova, M., 2018. Temporal analysis of the

434 autophagic and apoptotic phenotypes in *Leishmania* parasites. *Microb. Cell* 5, 404–417.
435 <https://doi.org/10.15698/mic2018.09.646>

436 Bastard, A., Coelho, C., Briandet, R., Canette, A., Gougeon, R., Alexandre, H., Guzzo, J.,
437 Weidmann, S., 2016. Effect of Biofilm Formation by *Oenococcus oeni* on Malolactic
438 Fermentation and the Release of Aromatic Compounds in Wine. *Front. Microbiol.* 7, 613.
439 <https://doi.org/10.3389/fmicb.2016.00613>

440 Bojsen, R., Regenber, B., Folkesson, A., 2014. *Saccharomyces cerevisiae* biofilm tolerance
441 towards systemic antifungals depends on growth phase. *BMC Microbiol.* 14, 305.
442 <https://doi.org/10.1186/s12866-014-0305-4>

443 Boucherit-Atmani, Z., Seddiki, S.M.L., Boucherit, K., Sari-Belkharoubi, L., Kunkel, D., 2011.
444 *Candida albicans* biofilms formed into catheters and probes and their resistance to
445 amphotericin B. *J. Mycol. Med.* 21, 182–187. <https://doi.org/10.1016/j.mycmed.2011.07.006>

446 Bridier, A., Sanchez-Vizuete, P., Guilbaud, M., Piard, J.C., Naïtali, M., Briandet, R., 2015.
447 Biofilm-associated persistence of food-borne pathogens. *Food Microbiol.* 45, 167–178.
448 <https://doi.org/10.1016/j.fm.2014.04.015>

449 Bruvo, R., Michiels, N.K., D’Souza, T.G., Schulenburg, H., 2004. A simple method for the
450 calculation of microsatellite genotype distances irrespective of ploidy level. *Mol. Ecol.* 13,
451 2101–2106. <https://doi.org/10.1111/j.1365-294X.2004.02209.x>

452 Chatonnet, P., Dubourdieu, D., Boidron, J., Pons, M., 1992. The origin of ethylphenols in wines.
453 *J. Sci. Food Agric.* 60, 165–178. <https://doi.org/10.1002/jsfa.2740600205>

454 Citiulo, F., Moran, G.P., Coleman, D.C., Sullivan, D.J., 2009. Purification and germination of
455 *Candida albicans* and *Candida dubliniensis* chlamydospores cultured in liquid media.
456 *FEMS Yeast Res.* 9, 1051–1060. <https://doi.org/10.1111/j.1567-1364.2009.00533.x>

457 Coenye, T., Nelis, H.J., 2010. *In vitro* and *in vivo* model systems to study microbial biofilm

458 formation. *J. Microbiol. Methods* 83, 89–105. <https://doi.org/10.1016/j.mimet.2010.08.018>

459 Conterno, L., Joseph, C.M.L., Arvik, T.J., Henick-kling, T., Bisson, L.F., 2006. Genetic and
460 Physiological Characterization of *Brettanomyces bruxellensis* Strains Isolated from Wines.
461 *Am. J. Enol. Vitic.* 57, 139–147.

462 Costerton, J.W., Lewandowski, Z., Caldwell, D.E., Korber, D.R., Lappin-Scott, H.M., 1995.
463 Microbial Biofilms. *Annu. Rev. Microbiol.* 49, 711–745.
464 <https://doi.org/10.1146/annurev.mi.49.100195.003431>

465 Daniels, K.J., Park, Y.N., Srikantha, T., Pujol, C., Soll, D.R., 2013. Impact of environmental
466 conditions on the form and function of *Candida albicans* biofilms. *Eukaryot. Cell* 12, 1389–
467 1402. <https://doi.org/10.1128/EC.00127-13>

468 Davey, M.E., O’toole, G.A., 2000. Microbial Biofilms: from Ecology to Molecular Genetics.
469 *Microbiol. Mol. Biol. Rev.* 64, 847–867. <https://doi.org/10.1128/MMBR.64.4.847-867.2000>

470 Flemming, H.-C., 2016. EPS—Then and Now. *Microorganisms* 4, 41.
471 <https://doi.org/10.3390/microorganisms4040041>

472 Flemming, H.-C., Wingender, J., 2010. The biofilm matrix. *Nat. Rev. Microbiol.* 8, 623–633.
473 <https://doi.org/10.1038/nrmicro2415>

474 Fugelsang, K.C., 1997. Wine microbiology. New York: The Chapman and Hall Enology Library.

475 Germec, M., Turhan, I., Demirci, A., Karhan, M., 2016. Effect of media sterilization and
476 enrichment on ethanol production from carob extract in a biofilm reactor. *Energy Sources,*
477 *Part A Recover. Util. Environ. Eff.* 38, 3268–3272.
478 <https://doi.org/10.1080/15567036.2015.1138004>

479 Hall-Stoodley, L., Costerton, J.W., Stoodley, P., 2004. Bacterial biofilms: from the Natural
480 environment to infectious diseases. *Nat. Rev. Microbiol.* 2, 95–108.
481 <https://doi.org/10.1038/nrmicro821>

482 Ishchuk, O.P., Zeljko, T.V., Schifferdecker, A.J., Wisén, S.M., Hagström, Å.K., Rozpędowska,
483 E., Andersen, M.R., Hellborg, L., Ling, Z., Sibirny, A.A., Piškur, J., 2016. Novel
484 centromeric loci of the wine and beer yeast *Dekkera bruxellensis* CEN1 and CEN2. PLoS
485 One 11, e0161741. <https://doi.org/10.1371/journal.pone.0161741>

486 Jachlewski, S., Jachlewski, W.D., Linne, U., Bräsen, C., Wingender, J., Siebers, B., 2015.
487 Isolation of extracellular polymeric substances from biofilms of the thermoacidophilic
488 archaeon *Sulfolobus acidocaldarius*. Front. Bioeng. Biotechnol. 3, 123.
489 <https://doi.org/10.3389/fbioe.2015.00123>

490 Jones, S.K., Hirakawa, M.P., Bennett, R.J., 2014. Sexual biofilm formation in *Candida tropicalis*
491 opaque cells. Mol. Microbiol. 92, 383–398. <https://doi.org/10.1111/mmi.12565>

492 Joseph, C.M.L., Kumar, G., Su, E., Bisson, L.F., 2007. Adhesion and Biofilm Production by
493 Wine Isolates of *Brettanomyces bruxellensis*. Am. J. Enol. Vitic. 58, 373–378.

494 Kamvar, Z.N., Tabima, J.F., Grünwald, N.J., 2014. *Poppr*: An R package for genetic analysis of
495 populations with clonal, partially clonal, and/or sexual reproduction. PeerJ 2, e281.
496 <https://doi.org/10.7717/peerj.281>

497 Kolter, R., Greenberg, E.P., 2006. The superficial life of microbes. Nature 441, 300–302.
498 <https://doi.org/10.1038/441300a>

499 Kregiel, D., James, S.A., Rygala, A., Berłowska, J., Antolak, H., Pawlikowska, E., 2018.
500 Consortia formed by yeasts and acetic acid bacteria *Asaia* spp. in soft drinks. Antonie Van
501 Leeuwenhoek 111, 373–383. <https://doi.org/10.1007/s10482-017-0959-7>

502 Lattey, K.A., Bramley, B.R., Francis, I.L., 2010. Consumer acceptability, sensory properties and
503 expert quality judgements of Australian Cabernet Sauvignon and Shiraz wines. Aust. J.
504 Grape Wine Res. 16, 189–202. <https://doi.org/10.1111/j.1755-0238.2009.00069.x>

505 Lin, X., Heitman, J., 2005. Chlamydospore formation during hyphal growth in *Cryptococcus*

506 *neoformans*. Eukaryot. Cell 4, 1746–1754. <https://doi.org/10.1128/EC.4.10.1746-1754.2005>

507 Longin, C., Degueurce, C., Julliat, F., Guilloux-Benatier, M., Rousseaux, S., Alexandre, H.,
508 2016. Efficiency of population-dependent sulfite against *Brettanomyces bruxellensis* in red
509 wine. Food Res. Int. 89, 620–630. <https://doi.org/10.1016/j.foodres.2016.09.019>

510 Martin, S.W., Douglas, L.M., Konopka, J.B., 2005. Cell Cycle Dynamics and Quorum Sensing in
511 *Candida albicans* Chlamydo spores Are Distinct from Budding and Hyphal Growth.
512 Eukaryot. Cell 4, 1191–1202. <https://doi.org/10.1128/EC.4.7.1191-1202.2005>

513 Mayer, C., Moritz, R., Kirschner, C., Borchard, W., Maibaum, R., Wingender, J., Flemming, H.-
514 C., 1999. The role of intermolecular interactions: studies on model systems for bacterial
515 biofilms. Int. J. Biol. Macromol. 26, 3–16. [https://doi.org/10.1016/S0141-8130\(99\)00057-4](https://doi.org/10.1016/S0141-8130(99)00057-4)

516 Møretrø, T., Langsrud, S., 2017. Residential Bacteria on Surfaces in the Food Industry and Their
517 Implications for Food Safety and Quality. Compr. Rev. Food Sci. Food Saf. 16, 1022–1041.
518 <https://doi.org/10.1111/1541-4337.12283>

519 Navarathna, D.H.M.L.P., Pathirana, R.U., Lionakis, M.S., Nickerson, K.W., Roberts, D.D., 2016.
520 *Candida albicans* ISW2 regulates chlamydo spore suspensor cell formation and virulence *In*
521 *Vivo* in a mouse model of disseminated candidiasis. PLoS One 11, e0164449.
522 <https://doi.org/10.1371/journal.pone.0164449>

523 Nunes, J.M., Bizerra, F.C., Ferreira, R.C. e, Colombo, A.L., 2013. Molecular identification,
524 antifungal susceptibility profile, and biofilm formation of clinical and environmental
525 *Rhodotorula* species isolates. Antimicrob. Agents Chemother. 57, 382–389.
526 <https://doi.org/10.1128/AAC.01647-12>

527 Nweze, E.I., Ghannoum, A., Chandra, J., Ghannoum, M.A., Mukherjee, P.K., 2012.
528 Development of a 96-well catheter-based microdilution method to test antifungal
529 susceptibility of *Candida* biofilms. J. Antimicrob. Chemother. 67, 149–153.

530 <https://doi.org/10.1093/jac/dkr429>

531 O’Connell, H.A., Kottkamp, G.S., Eppelbaum, J.L., Stubblefield, B.A., Gilbert, S.E., Gilbert,
532 E.S., 2006. Influences of Biofilm Structure and Antibiotic Resistance Mechanisms on
533 Indirect Pathogenicity in a Model Polymicrobial Biofilm. *Appl. Environ. Microbiol.* 72,
534 5013–5019. <https://doi.org/10.1128/AEM.02474-05>

535 Oelofse, A., Pretorius, I.S., du Toit, M., 2008. Significance of *Brettanomyces* and *Dekkera* during
536 Winemaking: A Synoptic Review. *South African J. Enol. Vitic.* 29, 128–144.
537 <https://doi.org/10.21548/29-2-1445>

538 Ojeda-Robertos, N.F., Torres-Acosta, J.F.J., Ayala-Burgos, A.J., Sandoval-Castro, C.A., Valero-
539 Coss, R.O., Mendoza-de-Gives, P., 2009. Digestibility of *Duddingtonia flagrans*
540 chlamydo spores in ruminants: *in vitro* and *in vivo* studies. *BMC Vet. Res.* 5, 46.
541 <https://doi.org/10.1186/1746-6148-5-46>

542 Paradis, E., Claude, J., Strimmer, K., 2004. APE: Analyses of Phylogenetics and Evolution in R
543 language. *Bioinformatics* 20, 289–290. <https://doi.org/10.1093/bioinformatics/btg412>

544 Park, Y., Srikantha, T., Daniels, K.J., Jacob, M.R., Agarwal, A.K., Li, X., Soll, D.R., 2017.
545 Protocol for Identifying Natural Agents That Selectively Affect Adhesion, Thickness,
546 Architecture, Cellular Phenotypes, Extracellular Matrix, and Human White Blood Cell
547 Impenetrability of *Candida albicans* Biofilms. *Antimicrob. Agents Chemother.* 61, e01319-
548 17. <https://doi.org/10.1128/AAC.01319-17>

549 Poupault, P., 2015. Caractérisation des phénomènes de bio-adhésion à l’origine des altérations
550 des vins, in: *Proceedings of the 10th International Symposium of Enology of Bordeaux.*
551 *Vigne et vin publications internationales* (ed), Œno 2015, Bordeaux, France, pp. 234–237.

552 Renouf, V., Falcou, M., Miot-sertier, C., Perello, M.-C., de Revel, G., Lonvaud-Funel, A., 2006.
553 Interactions between *Brettanomyces bruxellensis* and other yeast species during the initial

554 stages of winemaking. J. Appl. Microbiol. 100, 1208–1219. <https://doi.org/10.1111/j.1365->
555 [2672.2006.02959.x](https://doi.org/10.1111/j.1365-2672.2006.02959.x)

556 Renouf, V., Lonvaud-Funel, A., 2007. Development of an enrichment medium to detect
557 *Dekkera/Brettanomyces bruxellensis*, a spoilage wine yeast, on the surface of grape berries.
558 Microbiol. Res. 162, 154–167. <https://doi.org/10.1016/j.micres.2006.02.006>

559 Renouf, V., Miot-sertier, C., Perello, M.-C., de Revel, G., Lonvaud-Funel, A., 2009. Evidence for
560 differences between *B. bruxellensis* strains originating from an enological environment. Int.
561 J. Wine Res. 1, 95–100. <https://doi.org/10.2147/IJWR.S4612>

562 Rieu, A., Aoudia, N., Jegou, G., Chluba, J., Yousfi, N., Briandet, R., Deschamps, J., Gasquet, B.,
563 Monedero, V., Garrido, C., Guzzo, J., 2014. The biofilm mode of life boosts the anti-
564 inflammatory properties of *Lactobacillus*. Cell. Microbiol. 16, 1836–1853.
565 <https://doi.org/10.1111/cmi.12331>

566 Rieu, A., Weidmann, S., Garmyn, D., Piveteau, P., Guzzo, J., 2007. *agr* system of *Listeria*
567 *monocytogenes* EGD-e: Role in adherence and differential expression pattern. Appl.
568 Environ. Microbiol. 73, 6125–6133. <https://doi.org/10.1128/AEM.00608-07>

569 Rubio, P., Garijo, P., Santamaría, P., López, R., Martínez, J., Gutierrez, A.R., 2015. Influence of
570 oak origin and ageing conditions on wine spoilage by *Brettanomyces* yeasts. Food Control
571 54, 176–180. <https://doi.org/10.1016/j.foodcont.2015.01.034>

572 Sauer, K., Camper, A.K., Ehrlich, G.D., Costerton, J.W., Davies, D.G., 2002. *Pseudomonas*
573 *aeruginosa* Displays Multiple Phenotypes during Development as a Biofilm. J. Bacteriol.
574 184, 1140–1154. <https://doi.org/10.1128/JB.184.4.1140>

575 Schifferdecker, A.J., Dashko, S., Ishchuk, O.P., Piškur, J., 2014. The wine and beer yeast
576 *Dekkera bruxellensis*. Yeast 31, 323–332. <https://doi.org/10.1002/yea>

577 Serpaggi, V., Remize, F., Recorbet, G., Gaudot-Dumas, E., Sequeira-Le Grand, A., Alexandre,

578 H., 2012. Characterization of the “ viable but nonculturable” (VBNC) state in the wine
579 spoilage yeast *Brettanomyces*. Food Microbiol. 30, 438–447.
580 <https://doi.org/10.1016/j.fm.2011.12.020>

581 Smith, B.D., Divol, B., 2016. *Brettanomyces bruxellensis*, a survivalist prepared for the wine
582 apocalypse and other beverages. Food Microbiol. 59, 161–175.
583 <https://doi.org/10.1016/j.fm.2016.06.008>

584 Son, H., Lee, J., Lee, Y.W., 2012. Mannitol induces the conversion of conidia to chlamyospore-
585 like structures that confer enhanced tolerance to heat, drought, and UV in *Gibberella zeae*.
586 Microbiol. Res. 167, 608–615. <https://doi.org/10.1016/j.micres.2012.04.001>

587 Staib, P., Morschhäuser, J., 2007. Chlamyospore formation in *Candida albicans* and *Candida*
588 *dubliniensis* - An enigmatic developmental programme. Mycoses 50, 1–12.
589 <https://doi.org/10.1111/j.1439-0507.2006.01308.x>

590 Stepanović, S., Vuković, D., Hola, V., Bonaventura, G. Di, Djukić, S., Circovic, I., Ruzicka, F.,
591 2007. Quantification of biofilm in microtiter plates: overview of testing conditions and
592 practical recommendations for assessment of biofilm production by Staphylococci. Apmis
593 115, 891–899. https://doi.org/10.1111/j.1600-0463.2007.apm_630.x

594 Suárez, R., Suárez-Lepe, J.A., Morata, A., Calderón, F., 2007. The production of ethylphenols in
595 wine by yeasts of the genera *Brettanomyces* and *Dekkera*: A review. Food Chem. 102, 10–
596 21. <https://doi.org/10.1016/j.foodchem.2006.03.030>

597 Tek, E.L., Sundstrom, J.F., Gardner, J.M., Oliver, S.G., Jiranek, V., 2018. Evaluation of the
598 ability of commercial wine yeasts to form biofilms (mats) and adhere to plastic: implications
599 for the microbiota of the winery environment. FEMS Microbiol. Ecol. 94.
600 <https://doi.org/10.1093/femsec/fix188>

601 Timke, M., Wang-Lieu, N.Q., Altendorf, K., Lipski, A., 2008. Identity, beer spoiling and biofilm

602 forming potential of yeasts from beer bottling plant associated biofilms. *Antonie Van*
603 *Leeuwenhoek* 93, 151–161. <https://doi.org/10.1007/s10482-007-9189-8>

604 Timke, M., Wolking, D., Wang-Lieu, N.Q., Altendorf, K., Lipski, A., 2004. Microbial
605 composition of biofilms in a brewery investigated by fatty acid analysis, fluorescence *in situ*
606 hybridisation and isolation techniques. *Appl. Microbiol. Biotechnol.* 66, 100–107.
607 <https://doi.org/10.1007/s00253-004-1601-y>

608 Tristezza, M., Lourenço, A., Barata, A., Brito, L., Malfeito-Ferreira, M., Loureiro, V., 2010.
609 Susceptibility of wine spoilage yeasts and bacteria in the planktonic state and in biofilms to
610 disinfectants. *Ann. Microbiol.* 60, 549–556. <https://doi.org/10.1007/s13213-010-0085-5>

611 Verstrepen, K.J., Klis, F.M., 2006. Flocculation, adhesion and biofilm formation in yeasts. *Mol.*
612 *Microbiol.* 60, 5–15. <https://doi.org/10.1111/j.1365-2958.2006.05072.x>

613 Wedral, D., Shewfelt, R., Frank, J., 2010. The challenge of *Brettanomyces* in wine. *LWT - Food*
614 *Sci. Technol.* 43, 1474–1479. <https://doi.org/10.1016/j.lwt.2010.06.010>

615 Zarnowski, R., Westler, W.M., Lacmbouh, G.A., Marita, J.M., Bothe, J.R., Bernhardt, J.,
616 Sahraoui, A.L.H., Fontainei, J., Sanchez, H., Hatfeld, R.D., Ntambi, J.M., Nett, J.E.,
617 Mitchell, A.P., Andes, D.R., 2014. Novel entries in a fungal biofilm matrix encyclopedia.
618 *MBio* 5, e01333-14. <https://doi.org/10.1128/mBio.01333-14>

619 Captions

620 **FIG 1** CLSM observations of 7 day-aged biofilms formed on polystyrene plates for the 12
621 selected strains. Cells were fluorescently tagged with cFDA. (A) For each strain (i) three-
622 dimensional reconstruction images of the biofilms generated a top view and side view, (ii)
623 zoomed-in images focus on cells and (iii) the thickness of biofilms. The images are
624 representatives of three independent biological replicates. (B) Filamentous cells in the biofilm
625 formed by strains 11 and 14.

626
627 **FIG 2** Distribution of the 12 strains selected according to length to width (l/w) ratio and cell area
628 measurements (CLSM images). The strains of each genetic group (GG) are represented by an
629 icon: (○) GG1, (▲) GG2, (■) GG3, (◇) GG4 and (◆) GG6. Clustering in 3 areas A, B and C
630 indicated by circles (ANOVA test and p-values ≤ 0.01).

631
632 **FIG 3** SEM observations of 7 day-aged microcolonies of strains 11 and 14 developed on stainless
633 steel chips in (A) YPD medium and (B) in wine. Magnifications were performed (i) at 500×:
634 development of the microcolonies on the stainless steel surface, (ii) at 3000×: filamentous cells
635 (indicated by white arrows), and (iii) at 7000×: microcolonies with EPS (indicated by white
636 arrows). The images are representatives of three independent biological replicates.

637
638 **FIG 4** Microcolony growth on stainless steel chips in wine for strains 11 and 14
639 ($\log_{10}(\text{CFU}/\text{cm}^2)$). Planktonic inoculum was expressed in CFU/mL. Errors bars represent the
640 standard deviation between three independent biological replicates. Statistical analysis is
641 performed between both strain at each time (ANOVA, p-value ≤ 0.05).

642 **FIG 5** Microcolony behavior in wine for (i) cells developed on the chips: (A) strain 11 and (B)
643 strain 14, (ii) cells released from biofilm into the wine: (C) strain 11 and (D) strain 14. Initial
644 populations were 1.1×10^6 CFU/cm² and 2.0×10^5 CFU/cm² respectively for strains 11 and 14.
645 Errors bars represent the standard deviation between three independent replicates. A different
646 letter indicates a significant difference (ANOVA, p-value ≤ 0.05).

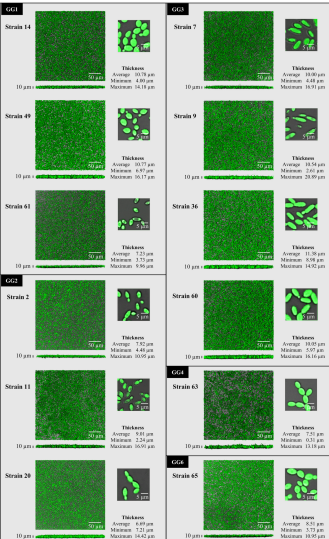
647
648 **FIG 6** Microscopic observations of “chlamyospore-like” structures produced by *B. bruxellensis*
649 in wine. (A) SEM observations (magnification at 7000×) of 14 day-aged microcolonies

650 developed on stainless steel chips in wine. (B) Epifluorescence microscopy observations after
651 calcofluor staining of adapted planktonic cell cultures of strains 11 and 14 in wine for 14 days.
652 White arrows indicate a “chlamyospore-like” structure.

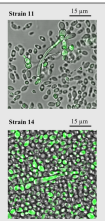
653

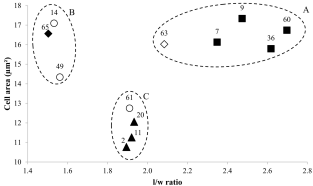
654

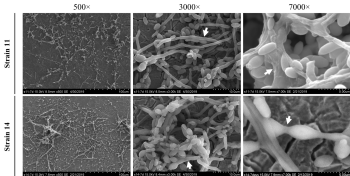
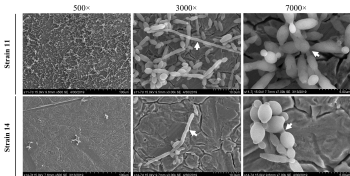
A



B

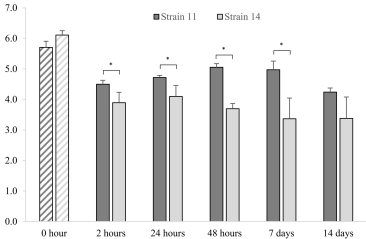


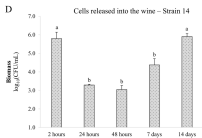
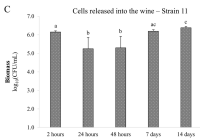
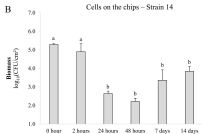
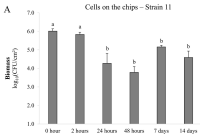


A**YPD medium****B****Wine**

Biomass

$\log_{10}(\text{CFU/mL})$
 $\log_{10}(\text{CFU/cm}^2)$





A**Strain 11****B****Strain 11****Strain 14**

1 **TABLE 1** Distribution of the 65 isolates among 34 clonal groups in the 6 genetic groups (GG)
 2 described by Avramova et al., 2018a. None of the isolates belonged to the GG5.

3

Genetic groups	Clonal groups (isolates)					
GG1	1					
	14					
	25	27	49			
	26	30				
	61	62				
GG2	2					
	4	6	11	17	19	
	20					
	3	10				
	5	42				
GG3	7	54	28			
	8					
	9	44	55			
	12					
	13	15				
	16					
	18	38	46			
	21	22	23	29	34	35
	24	37				
	31					
	32	52	53			
	33					
	36	40	43	64	47	48
	41					
	45					
	50					
	51					
	56					
	57					
58						
59						
60						
GG5	-					
GG4	63					
GG6	65					

4

5 **TABLE 2** Biofilm growth of the 12 selected strains in YPD medium on polystyrene plates.
6 Cultures were initially inoculated at 5.0×10^5 CFU/mL. The values represent the average of three
7 independent biological replicates, assigned with standard deviation (gray values). Different letters
8 represent significant difference (ANOVA, p -value ≤ 0.05) obtained between the 12 strains at each
9 time point.

10

Strain	CFU/cm ²								
	48 hours			7 days			14 days		
2	3.9×10^6	$\pm 2.68 \times 10^5$	a	6.1×10^6	$\pm 9.69 \times 10^5$	a	3.2×10^6	$\pm 1.88 \times 10^5$	ab
7	3.6×10^6	$\pm 5.53 \times 10^5$	a	2.5×10^6	$\pm 5.87 \times 10^5$	d	6.3×10^6	$\pm 1.16 \times 10^6$	a
9	3.1×10^6	$\pm 9.45 \times 10^5$	a	2.3×10^6	$\pm 1.54 \times 10^5$	d	4.7×10^6	$\pm 1.14 \times 10^6$	a
11	7.5×10^5	$\pm 2.15 \times 10^5$	bc	6.9×10^5	$\pm 5.11 \times 10^4$	e	2.4×10^6	$\pm 1.02 \times 10^6$	b
14	2.1×10^6	$\pm 1.47 \times 10^6$	ab	8.9×10^5	$\pm 1.62 \times 10^5$	e	5.3×10^6	$\pm 6.50 \times 10^5$	a
20	6.5×10^5	$\pm 9.99 \times 10^4$	c	2.8×10^6	$\pm 6.93 \times 10^5$	cd	5.4×10^6	$\pm 7.02 \times 10^5$	a
36	2.9×10^6	$\pm 6.93 \times 10^5$	a	3.3×10^6	$\pm 5.81 \times 10^5$	bcd	5.9×10^6	$\pm 2.57 \times 10^6$	a
49	4.6×10^6	$\pm 1.44 \times 10^6$	a	3.6×10^6	$\pm 2.92 \times 10^5$	abcd	3.3×10^6	$\pm 1.02 \times 10^6$	ab
60	6.6×10^5	$\pm 2.02 \times 10^5$	c	5.5×10^6	$\pm 1.41 \times 10^6$	ab	3.4×10^6	$\pm 7.47 \times 10^5$	ab
61	3.1×10^6	$\pm 7.36 \times 10^5$	a	4.5×10^6	$\pm 6.78 \times 10^5$	abc	3.2×10^6	$\pm 3.43 \times 10^5$	ab
63	1.5×10^5	$\pm 6.10 \times 10^4$	d	3.0×10^6	$\pm 8.87 \times 10^5$	cd	4.2×10^6	$\pm 5.62 \times 10^5$	ab
65	3.8×10^6	$\pm 1.35 \times 10^5$	a	6.3×10^6	$\pm 2.36 \times 10^5$	a	3.5×10^6	$\pm 6.44 \times 10^5$	ab

11

12 **TABLE 3** Average values of cell area and of length to width (l/w) ratio and shape of the cells for
 13 the 12 selected strains obtained from CLSM images.

14

Strain	Average l/w	Average cell area (μm^2)	Shape	
GG1	14	1.53 \pm 0.19	17.10 \pm 2.55	Round
	49	1.56 \pm 0.18	14.34 \pm 2.39	Round
	61	1.91 \pm 0.30	12.75 \pm 2.63	Rice grain
GG2	2	1.89 \pm 0.25	10.77 \pm 2.44	Rice grain
	11	1.92 \pm 0.42	11.26 \pm 3.49	Rice grain
	20	1.93 \pm 0.27	12.06 \pm 2.15	Rice grain
GG3	7	2.35 \pm 0.42	16.13 \pm 2.82	Elongated
	9	2.47 \pm 0.31	17.34 \pm 3.08	Elongated
	36	2.62 \pm 0.46	15.79 \pm 2.75	Elongated
	60	2.70 \pm 0.51	16.74 \pm 3.24	Elongated
GG4	63	2.08 \pm 0.47	16.03 \pm 2.79	Lemon
GG6	65	1.50 \pm 0.20	16.57 \pm 3.32	Round

15